10.1109/ULTSYM.2010.0145

Spatial Compounding for 2D Strain Estimation in the Mouse Heart: a Pilot Study

Florence Kremer*, Muna Rabayah*, Hon Fai Choi*, Matilda Larsson* † and Jan D'hooge * ‡
* Lab on Cardiovascular Imaging and Dynamics, Department of Cardiovascular Diseases,
Katholieke Universiteit Leuven, Leuven, Belgium
† School of Technology and Health, Royal Institute of Technology, Stockholm, Sweden
‡ MI lab, Norwegian Institute for Science and Technology, Trondheim, Norway
Email: florence.kremer@uz.kuleuven.ac.be

***Abstract*—Estimating cardiac strain in the mouse in the lateral direction using speckle tracking with adapted clinical equipment was shown to be challenging due to the fast heart rate and the large speckle size relative to the wall thickness. Compounding axial motion estimates acquired from different insonation angles can potentially improve lateral strain estimates. Therefore, the aim of this study was to test the feasibility of this methodology in the murine heart based on simulated data sets.**

A 3D kinematic model of a murine left ventricle was simulated and filled randomly with scatterers. Ultrasound short-axis images (10mm x 6mm) were obtained by assuming a linear array transducer. Beam steering was simulated at 3 different angles (22°, 0°, -22°). Axial motion was estimated in each data set by 1D cross-correlation. A dynamic programming approach was integrated in the motion estimation algorithm to avoid discontinuities. Axial components were combined to reconstruct the in-plane motion vector. The 2D displacement fields were subsequently accumulated over the whole cycle. The procedure was repeated for 10 different distributions of scatterers to acquire 10 different RF data sets (5 for parameter tuning and 5 for comparing the methods).

Radial and circumferential RMS strain errors calculated from the accumulated motion fields were compared with those obtained with 2D speckle tracking. Spatial compounding yielded significantly better radial (RMSE: 0.0737 ± 0.0078 vs. 0.112 ± 0.0094) as well as circumferential strain (RMSE: 0.102 ± 0.0097 vs. 0.281 ± 0.054).

I. Introduction

Small animal models are of great interest in cardiovascular research since they allow to understand how genetic defects are related to disease [1]. As such, extensive phenotyping of these animal models is of primary interest. In humans, different methods have been developed for the quantification of regional myocardial function using ultrasound, such as Doppler myocardial imaging and more recently, 2D speckle tracking. Consequently, adapting these methods to the small animal setting would be of relevance. However, direct translation of 2D speckle tracking to the murine setting is challenging because of the small size and the fast heart rate of the murine heart. In an previous study, it was shown that mainly lateral motion estimates (perpendicular to the ultrasound beam) need to be improved [2]. This problem is not straightforward as it is due to the lateral resolution of the system itself (i.e the lack of phase information in that direction and the larger speckle size compared to the wall thickness).

Compounding axial motion estimates obtained from at least 2 acquisitions with different insonation angles can potentially improve lateral strain estimates. Feasibility of this technique was established in-silico as well as in-vitro [3],[4],[5]. Recently, Hansen *et al*. tested beam steering in vessel phantoms and showed that the compounding method outperformed 2D RF-based speckle tracking [6]. Therefore, the aim of this study was to analyse whether the compounding of 1D axial motion estimates could possibly improve 2D strain estimation in the murine heart using simulated data sets.

II. Methods

A. Data simulation

A kinematic ellipsoid model of a mouse left ventricle (LV) with realistic dimensions and properties (Ejection fraction 60%, wall thickness 0.8mm, short axis diameter 4mm, long axis length 6mm and heart rate 577bpm) was constructed and filled with a random distribution of point scatterers at a density of 5000 per mm^3. Short axis ultrasound data sets with a field of view (FOV) of 10 mm x 6 mm at the middle level of the heart were simulated based on a previously described methodology [7] using a linear array transducer transmitting at a center frequency of 15MHz, with a sampling frequency of 200MHz, an overlap between beams of 95% and a frame rate of 300Hz. The corresponding axial and lateral spatial resolutions were 77 x 475 μm respectively. Images were simulated for different angles (-22°, 0°, 22°) using beam steering. These angles and FOV were chosen to be similar to what is typically obtained in commercially available scanners. The whole procedure was repeated for 10 different distributions of scatterers. Five radio-frequency (RF) data sets were used for tuning the parameters and 5 for testing the motion estimation algorithm.

B. Motion estimation

1) 2D Speckle tracking (2D ST): Motion was estimated on the RF signal by tracking a 2D kernel between subsequent frames using the normalized cross correlation algorithm as similarity measure. A cubic spline was then fit through the correlation function to achieve sub-sample resolution. All estimations were performed with 40% axial and no lateral overlap between kernels, a kernel size of 2 x 5 wavelengths (λ = 0.1mm), and assuming a maximum velocity of 6 cm/s.

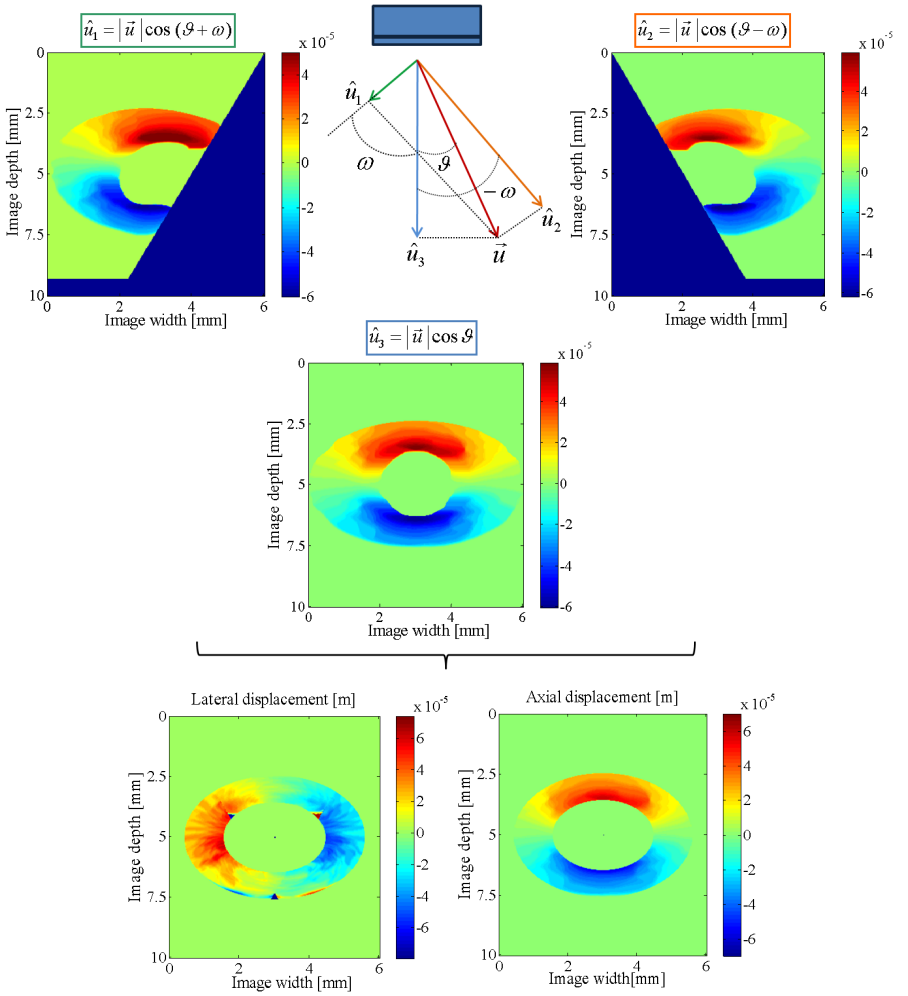

Fig. 1. Example of axial motion estimates obtained from the 22°-angle (above left), the 0°-angle (above in the middle) and the -22°-angle (above right) acquisition at the end of the systole. The corresponding lateral (below left) and axial (below right) motion estimates are derived from these 3 acquisitions.

These parameters were chosen based on a preliminary study (data not shown). Motion assessment was followed by 2D median filtering on a region of 0.25 x 1mm and by linear interpolation between samples in both directions in order to obtain an estimate in each pixel of the B-mode image.

2) 1D motion estimation: Motion along the beam direction (axial motion) was estimated on each RF line using similar parameters as for 2D ST: normalized cross correlation, a kernel length of 2λ, an overlap of 40% and a 1D search region that allowed for a maximal velocity of 6 cm/s. In order to avoid peak hopping artifacts, dynamic programming was integrated in the motion estimation algorithm in the same way as described in Petrank *et al* [8]. Parameters of the dynamic programming algorithm were tuned on the 5 training data sets. After that, the 1D motion estimates were linearly interpolated to the initial resolution. As for 2D ST, median filtering on a region of size 0.25 x 1mm was performed on the 2D displacement field.

C. Compounding axial estimates from 3 tilted acquisitions

First, axial displacement fields coming from the 3 acquisitions were expressed in the same coordinate system (0°-angle coordinate system) through bilinear interpolation. Then, motion perpendicular to the beam line (lateral motion) was reconstructed as shown in Figure 1. Hereto, each measured axial motion was written as the projection of the real motion vector field on the ultrasound line. For each point in the tissue, this is expressed as follows:

$$\hat{u}_{ax\ \omega} = |\vec{u}|\ cos(\theta + \omega) \qquad (1)$$

with $|\vec{u}|$ the amplitude of the true motion vector $\vec{u}$ and θ its angle with the 0° axis, while $\hat{u}_{ax\ \omega}$ being the axial motion component measured from the ω-tilted acquisition. Equation (1) expressed for each angle can thus provide a set of equations that can be solved for the 2 unknowns $|\vec{u}|$ and θ.

In order to obtain axial motion fields, the 0°-angle estimates were used as such without further processing. It was indeed shown that axial motion would benefit from the

other components only if the steering angle is less than 4° [5].

As not all the tilted frames can cover the whole field of view, there is a region where only one estimate is available (from the 0°-angle acquisition). This region is located in the inferior wall. Only the axial component can be measured there. On the countrary, the anterior wall is covered by all 3 tilted acquisitions. In that case, the measurements coming from the 2 furthest angles (i.e. ω and $-\omega$) were considered since they are supposed to give less noisy results.

D. Accumulation

For both methods, lateral and axial displacement fields were accumulated throughout the complete cardiac cycle. To do so, end diastolic pixel centers were tracked from one frame to the next by using bilinear interpolation to take subpixel motion into account.

E. Strain calculation

In order to obtain radial and circumferential strain which are more relevant in cardiology, the accumulated displacement fields were converted to polar coordinates, with the origin of the coordinate system being located in the center of the image. Normal strains in the radial direction ϵ_{rr} and in the circumferential direction $\epsilon_{\theta\theta}$ were calculated at 20 equally spread circumferential positions in the middle of the wall as follows:

$$\epsilon_{rr} = \frac{\Delta u_r}{\Delta r} \tag{2}$$

$$\epsilon_{\theta\theta} = \frac{1}{r}(\frac{\Delta u_\theta}{\Delta \theta} + u_r) \tag{3}$$

with the displacement field being referred to as $\mathbf{u} = (u_r, u_\theta)$.

Because non-zero strains at the end of the cardiac cycle are physiologically not possible, drift of the strain curve was corrected. The drift-compensated strains ϵ' at position $\mathbf{x}$ and frame t were calculated as follows:

$$\hat{\epsilon}(\mathbf{x}, t) = \epsilon(\mathbf{x}, t) - \frac{\sum_{i=1}^{t} |\epsilon(\mathbf{x}, i) - \epsilon(\mathbf{x}, i-1)|}{\sum_{j=1}^{T} |\epsilon(\mathbf{x}, j) - \epsilon(\mathbf{x}, j-1)|} \epsilon(\mathbf{x}, T), \tag{4}$$

with frame 1 the first end diastolic frame and frame T the second end diastolic frame.

F. Error measure

In order to analyse the performance of the algorithm, the RMS strain error ξ_S and the RMS displacement error through time $\xi_D(t)$ were defined as:

$$\xi_S = \sqrt{\sum_{k=1}^{N} \frac{\sum_{t=1}^{M} [\hat{\epsilon}(\mathbf{x_k}, t) - \epsilon_{true}(\mathbf{x_k}, t)]^2 / M}{N}} \tag{5}$$

$$\xi_D(t) = \sqrt{\sum_{k=1}^{P} \frac{[\hat{u}(\mathbf{x_k}, t) - u_{true}(\mathbf{x_k}, t)]^2}{P}} \tag{6}$$

with $\mathbf{x}$ standing for a position in the tissue, M for the number of frames, N for the number of locations considered for strain calculation ($N = 20$) and P the number of pixels in the image, while ϵ_{true} and u_{true} denote the true strain and the true displacement field respectively. A paired t-test was then carried out on radial and circumferential RMS strain errors ξ_S. A p-value less than 0.05 was considered statistically significant.

III. Results

Figure 2 shows the lateral and axial RMS displacement error profile $\xi_D(t)$ during one cardiac cycle for both methods and averaged over the 5 test data sets. The statistical analysis on the RMS strain error ξ_S is presented in Figure 3. All p-values were smaller than 0.001.

IV. Discussion

Axial displacement errors were similar for 2D ST and 1D compounding throughout the cardiac cycle except for the filling and ejection phase. In these periods velocities are relatively high which showed to have more impact on the accuracy of the 2D ST approach. As such, spatial compounding outperformed 2D ST during these periods.

Lateral motion estimation was better throughout the cardiac cycle when using 1D compounding. This finding is in agreement with previous studies [6] and confirms that compounding can improve the accuracy of 2D motion estimation in the murine heart when using commercially available clinical equipment. As expected, these better motion estimates also resulted in more accurate estimates of both myocardial strain components (Figure 3).

In this study, an implementation of 2D-ST specifically developed for murine myocardial strain estimation was used. Obviously, better tracking algorithms might be developed and more accurate measurements could be obtained through further regularization of the 2D motion estimates [2]. As such, improved 2D-ST algorithms might outperform 1D compounding. However, the same holds true for the 1D compounding technique used in this study that could further be optimized. As basic algorithms were used for both 2D-ST and for 1D-compounding, it thus seems reasonable to believe that these findings would hold for more advanced algorithms as well.

1D motion estimation was done through cross-correlation with subsequent filtering to avoid peak hopping. This is not realistic for current state-of-the-art commercial equipment that typically uses auto-correlation based motion estimators. However, as the main goal of this study was to test the performance of 1D compounding with respect to 2D ST, this was not considered important as the findings presented here should hold.

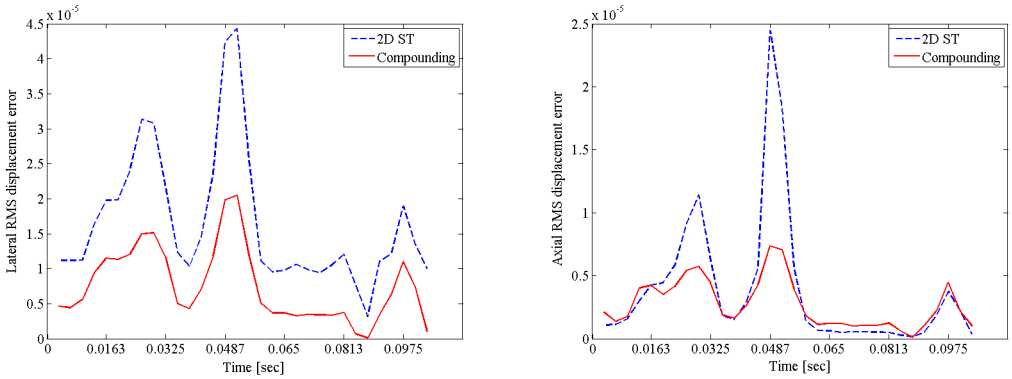

Fig. 2. Comparison of lateral (left) and axial (right) RMS displacement errors obtained either with 2D speckle tracking (dashed) or with spatial compounding (solid) during one cardiac cycle. RMS errors were averaged over the 5 test data sets.

Lateral displacement estimates obtained by 1D compounding were noisy close to the borders of the myocardial model (Figure 1). This was attributed to zero padding in the 2D median filtering process. However, as strain was calculated in the middle of the myocardial wall, this should have minimal effect on the results presented.

Obviously, 1D compounding requires multiple acquisitions which lengthens the acquisition time. However, as murine heart rates are very high and as all acquisitions can be done through beam steering while keeping the position and orientation of the transducer fixed, this increase in acquisition time would remain limited and, as such, not form a practical obstacle of using such an approach.

Finally, it should be noted that compounding was not possible in a small part of the inferior wall as the field of views of the different acquisitions were not overlapping in this area. Obviously, the extent of this region is dependent on several parameters such as insonation angle, field of view, position and size of the heart. In this study, all parameters were chosen realistic and according to specifications of available commercial equipment in order to be able to apply this exact same methodology in vivo. Of course, some of the acquisition parameters could be optimized further to avoid these drop-out regions as much as possible.

V. Conclusion

This study shows that spatial compounding of 1D axial displacement fields can improve motion estimation compared to 2D speckle tracking in the challenging setting of the murine heart. In the future, the performance of the method will be tested in the in-vivo setting.

Acknowledgment

This work was supported by grant G.0684.08 of the Research Foundation - Flanders (FWO - Vlaanderen). Hon Fai Choi is a Research Assistant of the FWO - Vlaanderen.

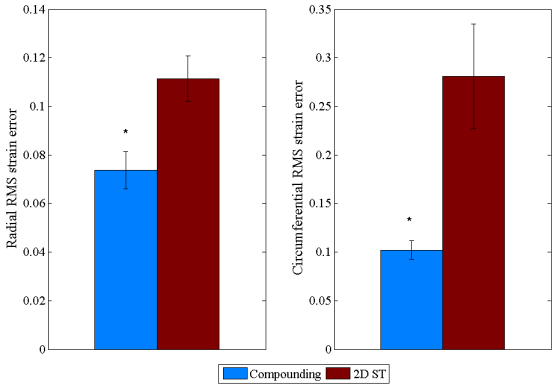

Fig. 3. Statistical analysis of radial (left) and circumferential (right) RMS strain errors obtained on 5 models either with 2D speckle tracking (left bar) or with spatial compounding (right bar) and averaged over one cardiac cycle. Significant differences are indicated by * ($p < 0.001$).

References

[1] James JF, Hewett TE, Robbins J. Cardiac Physiology in Transgenic Mice. Circ Res 1998;82:407-15.

[2] Kremer F, Choi HF, Claus P, Langeland S, D'Agostino E, D'hooge J Geometric Regularization for 2D Myocardial Strain Quantification in Mice: An In-Silico Study, Ultrasound Med Biol. 2010;36(7);1157-1168.

[3] Techavipoo U, Chen Q, T. Varghese T, Zagzebski JA. Estimation of Displacement Vectors and Strain Tensors in Elastography Using Angular Insonifications IEEE Trans Med Imaging, 2004;23(12):1479-1489.

[4] Rao M, Chen Q, Shi H, Varghese T, Madsen EL, Zagzebski JA, Wilson TA. Normal and Shear Strain Estimation Using Beam Steering on Linear-Array Transducers. Ultrasound Med Biol. 2007;33(1);57-66.

[5] Rao M, Varghese T. Estimation of the Optimal Maximum Beam Angle and Angular Increment for Normal and Shear Strain Estimation IEEE Trans Biomed Eng. 2009;56(3):760-769.

[6] Hansen HHG, Lopata RCP, Idzenga T, de Korte CL. Full 2D Displacement Vector and Strain Tensor Estimation for Superficial Tissue Using Beam-steered Ultrasound Imaging. Phys Med Biol, 2010;55:3201-3218.

[7] Gao H, Choi HF, Claus P, Boonen S, Jaecques S, Van Lenthe GH, Van der Perre G, Lauriks W, D'hooge J. A Fast Convolution-based Methodology to Simulate 2D / 3D Cardiac Ultrasound Images. IEEE Trans Ultrason Ferroelectr Freq Control 2009;56:404-409.

[8] Petrank Y, Huang L, Matthew O'Donnell, Reduced Peak-Hopping Artifacts in Ultrasonic Strain Estimation Using the Viterbi Algorithm, IEEE Trans Ultrason Ferroelectr Freq Control, 2009;56:1359-1367.